IIETA International Information and Engineering Technology Association
Advancing the World of Information and Engineering

Mathematical Modelling of Engineering Problems
Vol. 9, No. 6, December, 2022, pp. 1648-1658
Journal homepage: http://iieta.org/journals/mmep

Using Greenhouse Modelling to Identify the Optimal Conditions for Growing Crops in Northeastern Thailand

Sakkarin Wangkahart[1,2], Chaiyan Junsiri[3,4*], Aphichat Srichat[5], Sahassawas Poojeera[6], Kittipong Laloon[3], Kaweepong Hongtong[5], Phaiboon Boupha[7]

[1] Department of Innovation Engineering, Faculty of Engineering, Khon Kaen University, Khon Kaen 40002, Thailand
[2] Faculty of Management Science, Udon Thani Rajaphat Univesity, Udon Thani 41000, Thailand
[3] Department of Agricultural Engineering, Faculty of Engineering, Khon Kaen University, Khon Kaen 40002, Thailand
[4] Postharvest Technology Innovation Center, Science, Research and Innovation Promotion and Utilization Division, Office of the Ministry of Higher Education, Science, Research and Innovation, Bangkok 10400, Thailand
[5] Department of Mechanical Engineering, Faculty of Technology, Udon Thani Rajabhat University, Udon Thani 41000, Thailand
[6] Department of Mechanical Engineering, Ragamangala University of Technology Isan, Khon Kaen 40000, Thailand
[7] Department of Smart Electronics and Electric Vehicles, Faculty of Technology, Udon Thani Rajabhat University, Udon Thani 41000, Thailand

Corresponding Author Email: chaich@kku.ac.th

https://doi.org/10.18280/mmep.090626

Received: 11 August 2022
Accepted: 20 November 2022

Keywords:
protected agriculture, microclimate, CFD model, simulation

ABSTRACT

The most essential components in escort farming are the determination of airflow patterns and the distribution impact of microclimate temperature variables. The objective of this study is to use Computational Fluid Dynamics (CFD) models to ascertain the aerodynamic and thermal dynamics of protected agricultural greenhouses suitable for cultivation in tropical Northeastern crops of Thailand by defining differences in greenhouse layouts, specifically Gable Roof (GR), Curved Roof (CR), Saw tooth roof (SR), and Double roof (DR). The root means square error (RMSE) indicated that the factor determination of CFD modelling using the standard $k-\varepsilon$ turbulence model was satisfactory. In addition, they found that, at a significance level of 0.05, the average temperature in the greenhouses was statistically distinct based on the form of the back of the house and the location of the air input and outflow.

1. INTRODUCTION

Concerns about consumer food insecurity Climate change has a direct impact on future food demand [1]. Food shortage is a huge issue affecting the whole planet. Climate also influences agricultural yield and quality [2]. Due to its controllability and high productivity, protected agriculture is implemented. The worldwide greenhouse area is roughly 3.64 million hectares, based on statistical data [3]. In recent years, food production in greenhouses has increased rapidly [4]; consequently, food production in greenhouses is a promising strategy for future sustainability [5] growing plants in greenhouses that requires a comprehensive consideration of both design and workflow [6], as well as greenhouse heat transfer [7]. The ability to regulate the atmosphere within a house is contingent on the size of the house. Location and dimensions of air vents [8]. Previous research has shown that temperature flow model simulation Temperature, along with relative humidity, transpiration, photosynthesis, and CO_2 concentration [9], is one of the most influential factors [10, 11] influencing crop development all over the globe. region of the globe and may prolong the growing season year-round for great harvests. Consequently, the interior environment of each plant must be maintained at an appropriate level [12, 13]. Proper management of the greenhouse environment was closely tied to plant development to boost harvests by drastically lowering the difference in air temperature between the inside and outside [14]. Protected agriculture is used mostly to regulate parameters in the desert and tropical horticultural crops [15]. In addition, the indoor atmosphere must be designed. It has been discovered that airflow is the principal mechanism dispersing the inside environment. Using of CFD is a technique, it can visualize air flow to make it easier to understand the aerodynamics. The study has been used in a significant amount of greenhouse development and improvement research. for the distribution of parameters in a curved roof orientation for different climates, including comparisons between shapes, cladding materials, different orientations, thermal insulation, and heat storage utilized for independent cooling systems [16-23].

Verification of parameters the comparison of CO_2 concentrations [24]. Currently, the greenhouse system is being developed as a "smart home" by using environmental control management techniques [25]. Considering the distribution of solar radiation throughout the summer and winter [26], testing in wind tunnels to evaluate wind-driven ventilation with vents along the lines of solar radiation [27]. Additionally, parameters are monitored using greenhouse data. Experiments on plant growth monitoring (microclimate) [28]. In the agriculture sector, solar greenhouses are now the most popular type [29-31]. To increase agricultural production in the tropics and subtropics, it is necessary to utilize pad-fan cooling (PFC)

Optimizing energy utilization is dependent on analyzing crucial elements, such as fan height and wind velocity [32]. To improve the system for managing the greenhouse environment, the cooling effectiveness of the house wall and the research on heat movement were also conducted [33, 34]. Using a CFD model is used to determine the roof orientation of a home [35].

As a result of the research review, greenhouse cropping systems management requires CFD modelling. Currently, greenhouses continue to be used for plant cultivation in Thailand's tropical regions. In Northeastern Thailand's tropical climatic zone; however, there has been no research on on-site- and plant-appropriate greenhouse design. Greenhouses for producing high-value crops that need a regulated atmosphere are solely employed in large-scale agricultural companies, which are the copyright of entrepreneurs and not published to farmers. The ideal greenhouse model for producing high-value crops as a model for indigenous agriculture that can be generated to compete with large-scale agro-industry operators must be investigated.

Therefore, the aims of this study were to create a greenhouse model suited for growing crops in a raised container. The simulation of the greenhouse aerodynamic environment using CFD technology was conducted to determine the climate effect in greenhouses with different roof designs with airflow volume air vents in-out using local weather characteristics such as temperature and wind patterns for each simulation time. Moreover, CFD model validation for indoor aerodynamics environment analysis was simulated to determine the optimal model for use in tropical climate areas of Northeastern, Thailand.

2. MATERIALS AND METHODS

This research used CFD methods to predict the optimal environment for plant growth in the greenhouses designed. In the simulation, four house styles are chosen. Additionally, monitoring data was gathered by sensing the inside temperature and wind speed was measured. The CFD model is modified based on simulation findings to ensure that simulation results are correct. The environment is then assessed based on the CFD model's flow dynamics.

2.1 Greenhouse case study

Udon Thani province of northeastern Thailand is the subject of the investigation of the indoor environment. According to each greenhouse model, coordinates 32°18′23.1"N 122°36′ 52.5"W the target greenhouses for this research were plastic greenhouses with the following roof characteristics: Gable Roof (GR), Curved Roof (CR), Saw tooth roof (SR), and Double roof (DR) (Figure 1).

2.2 Computational Fluid Dynamics (CFD)

The use of CFD has grown widespread in engineering. Increasing numbers of researchers are using this method to analyze indoor air quality, animal husbandry and animal food production. Storage facilities to develop systems to manage interior climate [36] are a valid modelling tool for forecasting greenhouse climates and cheap prices. It has been shown that CFD is a reliable and inexpensive modelling approach for forecasting greenhouse climates with accurate findings [37]. Simulation of CFD is a technique for validating numerical findings. The most prevalent experimental technique consisted of measuring micro variables inside the examined structure. The most used software is Ansys Fluent, which parses and solves equations that describe the behaviour of airflow using a throttling mechanism. The most developed simulation was under steady-state conditions using Standard k-ε, with the majority of investigations calculating the home ventilation rate and temperature distribution [38]. CFD is a methodology that uses a volume approach to solve the finite volume method (FVM). Typically, the CFD model creation process consists of three parts. This comprises the phases of pre-processing, processing, and post-processing. Physical design to create grid mesh is developed in the pre-processing step. Solving nonlinear partial differential equations following the rule of conservation of mass, momentum, and energy yields the fluid flow and energy principles for the model. In the post-processing phase, qualitative and quantitative analyses of computational data were conducted [39]. This research used the ANSYS FLUENT software processing as well as post-processing.

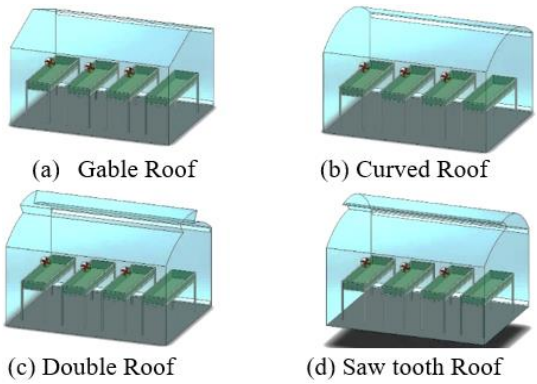

Figure 1. Greenhouse case study

2.3 CFD greenhouse model

2.3.1 Heat transfer and fluid flow equations

The CFD simulation solves the flow control equation for greenhouse fluid flow. The Navier-Stokes equation is derived by applying the second law of Newton to the fluid element [40].

$$\frac{\partial \rho \vec{U}}{\partial x} + \vec{U}\nabla\rho\vec{U} = -\nabla p + \mu\nabla^2\vec{U} + S_U \quad (1)$$

where, ρ is the dynamic viscosity, t the time, $\vec{U}$ the vector of velocity, whose x-component is u, p the pressure, μ dynamical turbulent viscosity and S_U the source of momentum.

Considerations for heat transfer and fluid flow. For shipyard fog cooling and dehumidification systems using the formula in free convention, the 3-D conservation equation for steady flow [41].

$$\frac{\partial(u*\varphi)}{\partial x} + \frac{\partial(v*\varphi)}{\partial y} + \frac{\partial(w*\varphi)}{\partial z} = \Gamma\cdot\nabla^2\varphi + S_\varphi \quad (2)$$

where, φ the 3-D momentum (Navier-Stokes) equation, as well as the scalar mass and energy conservation equations, reflect the concentration of the carried quantity in a dimensional form; x, y and z are the coordinates in Cartesian coordinates; u^* v^* and w^* are the reduced forms of the velocity vector's components; Γ is the coefficient of diffusion; ∇^2 is the operator Laplace; and S_φ is the original term.

2.3.2 Physical models and fundamental equations

The equations used in this model are as follows: A gathering of models for mass Eq. (3), momentum Eq. (4) and energy Eq. (5) from Navier-Stokes equations were solved with a model of realizable turbulence. The embedded turbulence model provides more precise airflow field distribution than the traditional turbulence model [42].

$$\frac{\partial \rho}{\partial t} + \nabla(\rho \vec{v}) = 0 \quad (3)$$

where, ρ is the density, t represents the time, and $\vec{v}$ is the velocity vector.

$$\frac{\partial}{\partial t}(\rho \vec{v}) + \nabla(\rho \vec{v}\vec{v}) = -\nabla P + \nabla \cdot (\overline{\tau}) + \rho \vec{g} \quad (4)$$

where, P is the pressure, $\overline{\tau}$ is the stress tensor, and $\vec{g}$ is the gravity acceleration.

2.3.3 Statistical analysis

All supplied parameters indicate the elements impacting the temperature in the greenhouse using the CFD approach for differentiation analysis of each house. One-Way ANOVA was used to assess the mean temperature findings for each residence. To examine the differences, the data were analyzed using a significance level of 0.05 and created a coefficient of correlation to demonstrate the temperature association between each house type.

2.4 CFD model validation greenhouse

The house for CFD model validation is located in Udon Thani. The northeast of Thailand. It is a greenhouse equipped with an environmental control system so that it may be assessed aerodynamically to evaluate the CFD model's validity in different forms without greenhouse cultivation to minimize the impact of external environmental factors. The examination session is in January 2022. The desired home dimensions are a gable-shaped construction measuring 3 meters broad, 4 meters long, 2 meters high eaves, and 2.5 meters high gable ridge. There is no sunshade on the translucent plastic cover with a thickness of 150 microns that reflects 7 per cent of UV radiation. High-Density Polyethylene infused with ultraviolet light is used to cover the floor of the home to avoid heat transmission from the ground. There is an air vent driven by a 10-inch exhaust fan located on the home's upper wall. The exhaust fan is activated by opening a vent on the opposite side of the house from the fan. Features ventilation holes, 10 cm wide, 4 m length.

By installing an air temperature sensor, the conditions for simultaneous monitoring of the aerodynamic environment in the greenhouse are created. and wind speed to collect data within the house. The information can be utilized to validate the CFD model. Points A, B, and C represent horizontal measurement points, whereas points 1 through 9 represent horizontal points. Environmental sensors were installed throughout the house at 27 points on three levels. Temperature, relative humidity, and wind speed may be determined by establishing a weather station at a height of 2 meters and sending data at 1-second intervals. The design of data storage is characterized in real-time (Real-Time). Microcontroller The smaller is the Node MCU ESP8266 V3 Temperature Humidity Sensor Module SHT20 with Typical accuracy (% RH) ±3 (°C) ±0.5. (Figure 2).

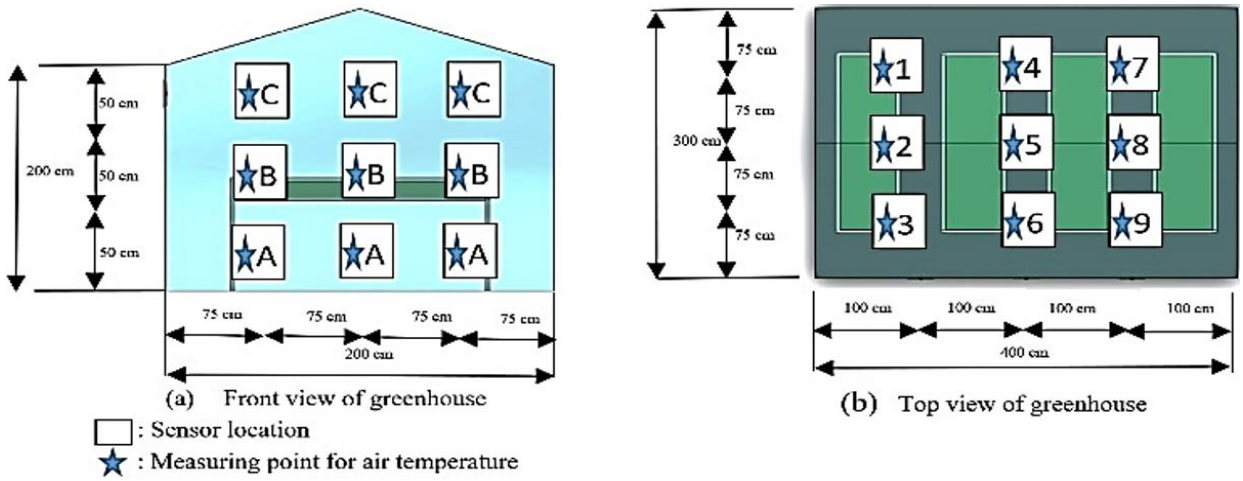

Figure 2. Sensor installation in the greenhouse for measuring air temperature and wind speed

Figure 3. Air temperature and wind speed measurements for CFD mode validation

Because of the unstable and unpredictable nature of weather, proper validation of the CFD model is difficult when a natural ventilation system is used. As a result, measurements were taken on a clear day from 11:00 a.m. to 4:00 p.m. using a mechanical ventilation system. (15 February 2022 - 24 February 2022) using the exhaust fan opening pattern. Before conducting temperature and air velocity measurements, the vents are closed to regulate the airflow throughout the greenhouse, then begin monitoring when the heat from solar radiation inside the house begins to stabilize. To start the measurement, switch on the fan and open the air inlet. When the inside airflow is steady five minutes after ventilation

begins, the indoor air temperature, the wall and floor temperatures, and the aerodynamic environment within the glasshouse are measured (Figure 3).

2.5 CFD simulation

Greenhouses for growing plants in the Northeastern region of Thailand. Due to environmental factors, there are many problems with the external environment. This study analyzes the problem by defining the representative of the environmental factors, and aerodynamic CFD simulation as Table 1.

Due to the environmental problem of excessive temperature in the selected agricultural region. To identify a technique to lower the temperature inside the glasshouse, the high-temperature issue was resolved by leveraging the ventilation system in the model greenhouse to generate the CFD model. To determine the most effective strategy, we must compare performance which is to utilize 1 exhaust fan and raise it incrementally until 3 side-wall units of 10 inches in diameter and 5 meters per second in wind speed are complete and compare the installation of the fan at 3 levels, namely, the top fan mounting point, measured from the edge of the eaves down 20 cm, the middle point of the side of the house and below 20 cm above the floor, as well as the determination of the inlet opening point, the size of 10 x 400 cm, set both in the opposite direction of the fan and on the opposite side of the fan at all 3 levels, with each house testing a total of 24 cases and four styles, there are a total of the total number of 96 cases.

Table 1. Case studies for aerodynamic environment analysis in greenhouses using CFD simulations

Conditions		Details	Cases
Greenhouse	Type	Gable Roof Curved Roof Double Roof Saw tooth Roof	4
Natural ventilation			
Air inlet	Square	10x400 cm	1
Air outlet	Circle	10 inches	1
Enter and exit from each side	Enter up the top area	Out of the upper section Out of the middle section out of the bottom section	3
	Enter out the lower box	Out of the upper section Out of the middle section out of the bottom section	3
Coming in and out of the same side	Enter up the top area	Out of the bottom section	1
	Enter out the lower box	Out of the upper section	1
Mechanical ventilation			
Number of fan (outlet)	1, 2, 3		3
Wind speed (m s^{-1})	5		1
(4) x (1 × 1 × 3 + 3 + 1 + 1) x (3x1) = 96 Cases			

2.6 Greenhouse mesh independence

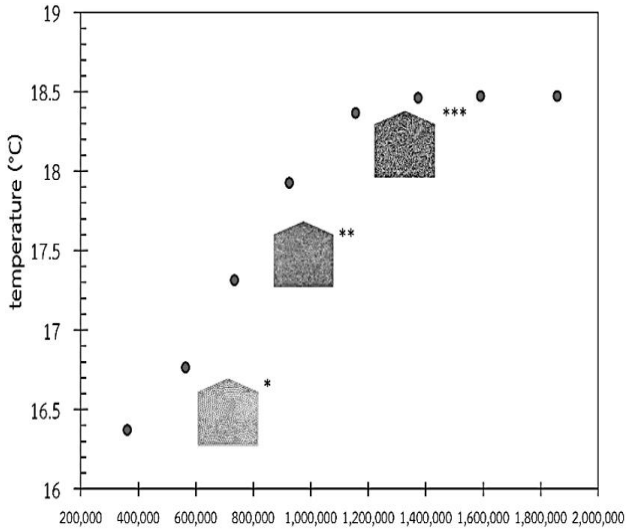

Figure 4. Establishing mesh independence

Creating mesh autonomy starts with creating reference case studies, such as a Case study with an input air temperature of 27 Celsius. Analyzing components into ever-smaller sizes and collecting the resulting number of elements allows each to examine the variation in the response factor's value. In the reference study, the output temperature was considered a reference factor when the reference factor was steady and the element division condition was used in subsequent analyses. The findings of the investigation indicate that the element size decreases until there are roughly 1.37×106 elements and the output temperature is steady. shown as indicated in Figure 4.

3. RESULTS AND DISCUSSION

3.1 CFD model validation findings for investigation of the aerodynamic environment in the greenhouse

Validation of the CFD model through comparison of data acquired in the greenhouse environment with simulation findings. The average absolute error ($\overline{v}$) and root mean square error (RMSE) can be calculated to evaluate the correctness of the observed data and from the simulation [43].

$$\overline{V} = \frac{1}{m}\sum_{i=1}^{m}\left|x_{pi} - x_{mi}\right| \quad (5)$$

$$RMSE = \sqrt{\frac{\sum_{m=1}^{m}(x_{p_i} - x_{mi})^2}{m}} \quad (6)$$

where, m is parameters' number; x_{pi} is simulated data; x_{mi} is measured data.

The purpose of the research was to compare variations in roof ventilation patterns across four variables, regardless of transpiration, photosynthesis, and particularly vegetative patterns. Consider how airflow influences changes in the indoor environment. As a result, the experiment was conducted using a gable-roof house as the principal building for testing, as this is the type most farmers in the area use. Validation of the validity and dependability of CFD models is required to provide adequate data. At heights A=50 cm, B=100 cm, and C=150 cm, temperatures were measured at 9 locations each layer for a total of 27 points. The values were determined to be RMSE=0.32℃ and 0.20℃ [44], who developed a model for comparable conditions and obtained an internal temperature of RMSE =1.6 K, and had a mean prediction error rate of 3.94 percent [45], indicating that the simulation values and actual values are comparable, so the CFD model has proven to be highly predictive. It may be utilized to analyze and explain the temperature and airflow distribution in the house (Figure 5).

3.2 CFD simulation results of aerodynamic environment in greenhouse

The results were examined using the Computational Fluid Dynamics (CFD) approach to determine the difference in average greenhouse temperatures as Table 2. Four housing models, GR, CR, SR, and DR were given, each with its air outlet/inlet design. There are 24 distinct designs. under the same conditions at the same temperature and humidity level, when the wind speed was 5 m s^{-1}, the air temperature was uniformly distributed throughout the greenhouse due to improved air mixing [46]. It was discovered that the GR house characteristics had a statistically significant difference in mean temperature for all types of houses (CR SR DR) at the 0.05 level [47]. The CR house style exhibited a statistically different mean temperature difference than the GR and DR house designs. Except for the SR house and the SR house, the mean temperature difference was statistically significantly different from the GR and DR home and the DR house. In terms of house style, the GR has the mean CFD house temperature, with a minimum internal temperature of 30.43℃ and a maximum of 30.59℃, while the CR has a minimum of 31.11℃ and a maximum of 34.01℃. 30.88℃ and a maximum of 33.34℃ and DR dwellings with a minimum internal temperature of 31.11℃ and a maximum internal temperature of 31.97℃ The gable roof home had the lowest mean temperature at 30.46℃, followed by the DR house with an average temperature of 31.42℃, the SR house with a mean temperature of 31.46℃, and the CR house with a mean temperature of 31.48℃ (Figure 6).

Table 2. Statistical comparative analysis to experiment with differences

Green House Type	Multiple Comparisons				Statistical Differentiations						
	GR	CR	SR	DR	Mean	Min	Max	S.D.	CV	F	p-Value
GR	1	-1.01483*	-.99639*	-.95402*	30.46	30.43	30.59	0.03	0.0010	2540.19	P< 0.05
CR		1	.01844	.06081*	31.48	31.11	34.01	0.30	0.0095		
SR			1	.04237*	31.46	30.88	33.34	0.33	0.0105		
DR				1	31.42	31.11	31.97	0.23	0.0073		

* The mean difference is significant at the 0.05 level

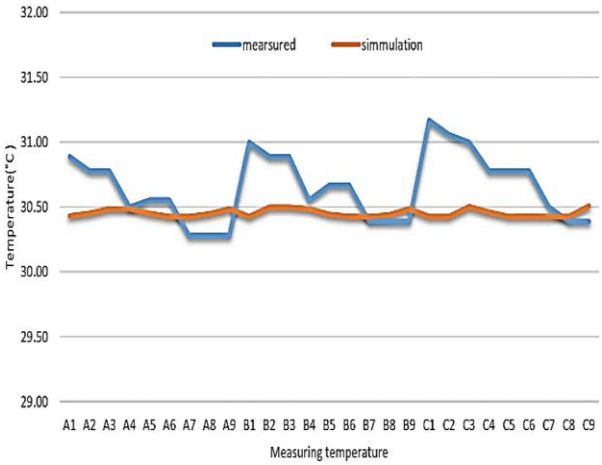

Figure 5. Validation of CFD models

Following that ventilation, wind speed, and humidity the majority of them are influenced by the form of the greenhouses and the size of the vents [48, 49].

When testing, the coefficient of variation (CV) is the ratio of the standard deviation to the mean [50]. It was discovered that the GR model house had the least variance distribution. It revealed that the temperature distribution was near to the mean house temperature, followed by DR, CR, and SR One-Way ANOVA analysis was used. The mean temperature in different roof shape buildings was statistically different ($p<0.05$) at the 95 % confidence level. Each component influences the temperature of the home This agrees with [51], who said that the air exchange rate is affected by the curvature of the roof.

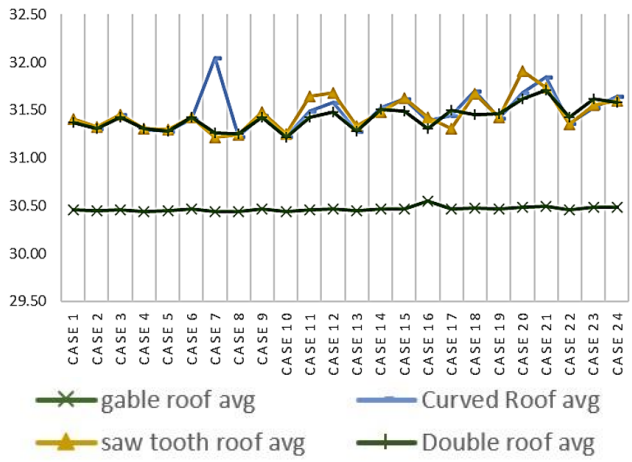

Figure 6. Temperature comparison in greenhouses

The 24 CFDs were performed on the GR housing layout. As indicated in Figure 7, air circulation and interior temperature resulted in the lowest mean air temperature within the house, which was 31.25℃. The average cross-sectional temperature

was 31.13℃ at A, 31.15℃ at B, and 31.46℃ at C, with air entering at the top and exiting at the bottom. As shown in Figure 7, the highest temperature is 32.35°C, which is the mean temperature of the cross-section, which is 32.15, 32.36, and 32.53℃, respectively. The average temperature was highest based on the preceding data and the lateral cross-section. The air with the highest temperature will rise to the roof of the house [52].

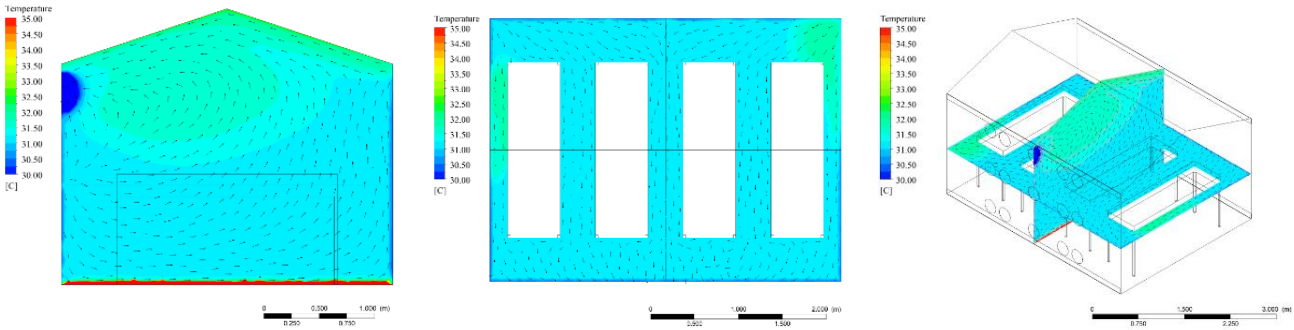

(a) Front view of greenhouse (b) Top view of greenhouse (c) Broad view

Figure 7. In the case of an upper air inlet air exit on top, a greenhouse-style gable roof is used (In and out of each side)

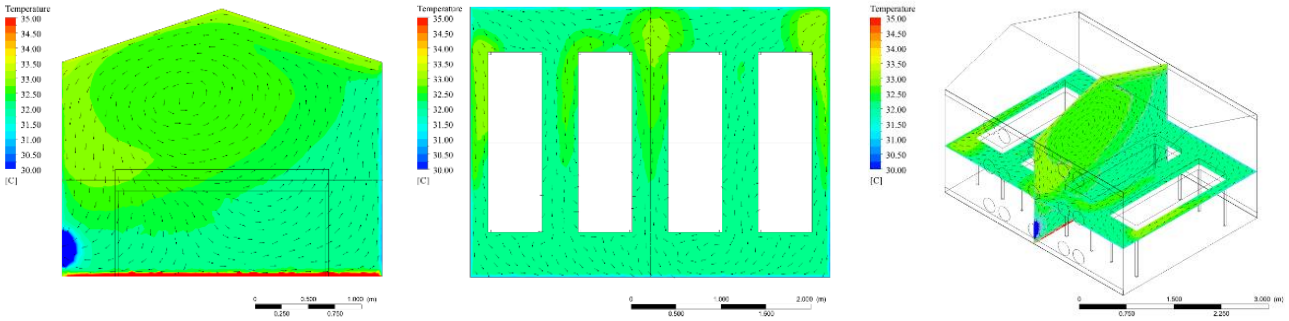

(a) Front view of greenhouse (b) Top view of greenhouse (c) Broad view

Figure 8. In the case of an upper air inlet and out below, a greenhouse-style gable roof is used (In and out of each side)

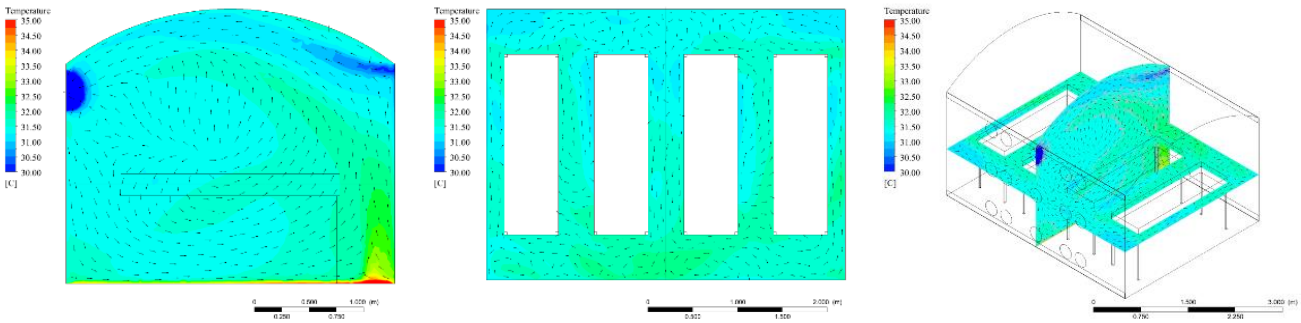

(a) Front view of greenhouse (b) Top view of greenhouse (c) Broad view

Figure 9. In the case of an upper air inlet air exit on top, a greenhouse-style curved roof is used (In and out of each side)

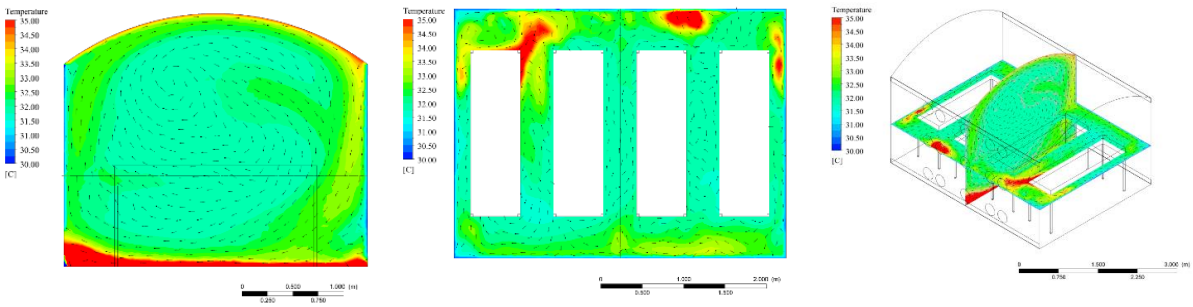

(a) Front view of greenhouse (b) Top view of greenhouse (c) Broad view

Figure 10. In the case of a lower air inlet and an air outlet below, a greenhouse-style curved roof is used (In and out of each side)

Figure 7(a) shows the colour scheme similarly. The high temperature rises to the top of the house and is then pushed to the exhaust fan by the natural air that enters the house. Consistent with the findings [53], Wind speed and direction have a considerable impact on a house's ventilation efficiency; the exhaust fan then exhausts the air from the dwelling. Furthermore, the existence of an aperture in the greenhouse's roof (a ridge) causes the temperature to drop and the velocity to increase [54]. When observing the direction of the arrow, it is apparent that the airflow below has a circular motion to the top of the house and will encourage incoming air from the outside to the fan's exhaust location.

The airflow in the area between the crop bed as seen in Figure 7(b), is directed through the crop bed generating heat from the bed while flowing in the direction of an arrow and rising as previously mentioned. In the case of the upper air inlet, the house must be chosen based on the experiment findings of all 24 GR houses, the house should be selected in the case of the upper air inlet, air outlet on top: which is suitable for practical use.

Due to the exhaust fan's position near the bottom of Figure 8, the rising air cannot reach the exhaust fan. As seen in Figure 8(a), some of them turn around and circle the house's centre after descending for a while. As shown in Figure 8(b), there are scattered, undirected motions along the sides of the crop bed, both downward and upward, followed by a circular motion in the house's centre. As previously noted, the high temperature cannot escape via the exhaust fan, causing the temperature that cannot be evacuated and receive higher temperature.

Figure 9 illustrates the upper airflow and upper air exit for the CR house, where the lowest mean air temperature was determined to be 31.23℃. The average cross-sectional temperatures at points A, B, and C are 31,13, 31,15, and 31,41 degrees Celsius, respectively. The C cross-section has the highest mean temperature, whereas Figure 9 shows the bottom air inlet and outlet, the highest mean temperature was 32.04℃, while the corresponding mean cross-sectional temperatures were 32.19, 32.02, and 31.92℃. Cross-section A has the highest temperature average.

In shaded colour as shown in Figure 9(a) heat rises to the top. The exhaust fan then pulls air out of the house, and the arrow tracing the air flow below moves in a round movement up the roof of the house. Increased wind speeds generate more homogeneous interior conditions and decrease turbulence levels [55, 56] which are caused by incoming air from the outside to the exit area ventilation.

As illustrated in Figure 9(b), the direction of airflow in the area between the crop bed is via the crop bed which generates heat from the crop bed. As mentioned earlier, the heat rises in a circle to the house's peak. Based on the experimental findings of the previously stated greenhouses, it is appropriate for future use.

Figure 10(a) illustrates a similar air vortex to those of Figure 10(b), with the exception that the heated shade circulates the walls along with the airflow, particularly the floor of the house, which has a higher temperature than other areas. The majority of temperature gradients occur close to the ground and roof [57, 58]. These transfers are mostly the result of radiation and convection transfer via walls and the ground [59].

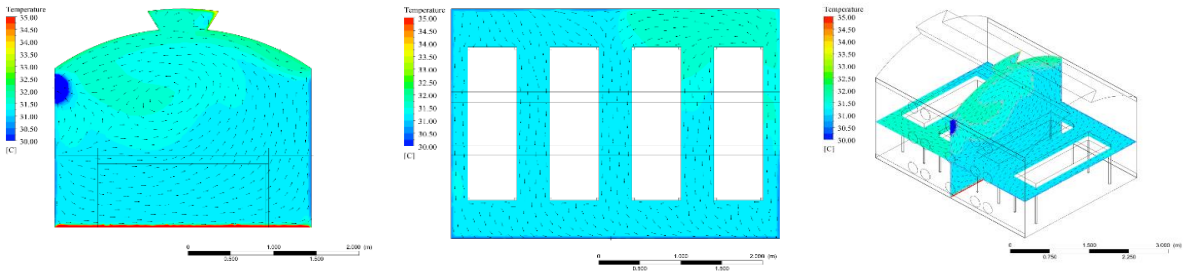

(a) Front view of greenhouse (b) Top view of greenhouse (c) Broad view

Figure 11. In the case of an upper air inlet and an air outlet above, a greenhouse-style double-roofed is used

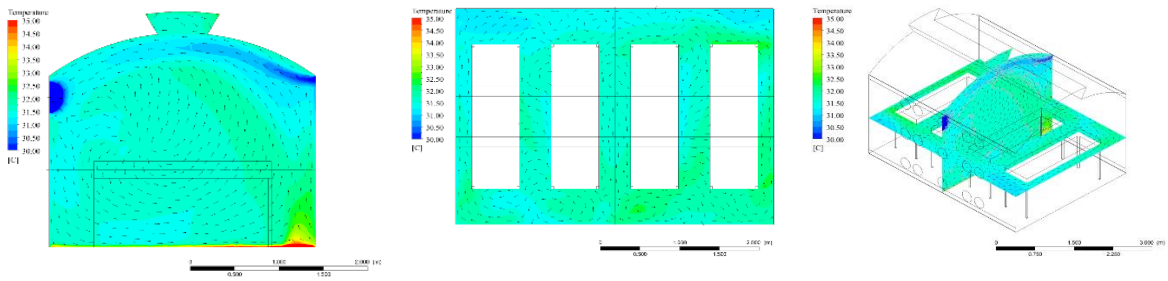

(a) Front view of greenhouse (b) Top view of greenhouse (c) Broad view

Figure 12. In the case of the top air inlet and three top outlets, a greenhouse-style double-roofed is used

The DR house has a natural flow between the house and the air inlet. In the instance of the upper air inlet and upper air outlet shown in Figure 11, the average temperature of the air inside the house was the lowest at 31.24℃, with mean cross-sectional temperatures of 31.14, 31.16, and 31.42℃. The cross-section at point C had the highest average temperature.

As shown in Figure 11, the greatest mean air temperature in the home was 31.68℃, with average cross-sectional temperatures of 32.67, 32.68, and 32.67℃ for the three higher air inlets and upper air outlets, respectively. The mean temperature is highest in cross-section B. From both situations, it is noticeable that the temperature in the home is highest in the high cross-section. Similarly, the colour scheme Figure 11(a) illustrates how air is pushed to the opposite side of the

house until it is taken out and replaced with outside air recirculated in the direction of the arrow. Ventilation and outside air flow affect ventilation efficiency [60].

Figure 11(b) The crop bed's airflow distributes warmth evenly throughout the house. Therefore, in the instance of the DR home model, the top air inlet and air outlet are the most practical structure. In the instance of three air inlets and outlets at the top, Figure 12(a) illustrates the structure Airflow direction in the area between the crop bed. The centre of the house is surrounded by a whirl of heated air. Under the crop bed, the air is flowing downward. High temperatures condensed below the inlet and were maintained up by the wind to circulate underneath the roof vents, where they are naturally vented by thermal floating on the two roof openings and maintain a constant temperature [61]. By increasing the roof ventilation area, the average inside temperature is reduced by 16%. Temperature consistency and raise the ventilation rate to 191% [62].

Figure 12(b) The temperature has a direction of scattering. There is no directional indication on the pickup truck's side. As indicated before, each has a downward and an upward path before circling the house's centre. This prevents the high temperature from escaping via the exhaust fan, thus the internal temperature continues to rise.

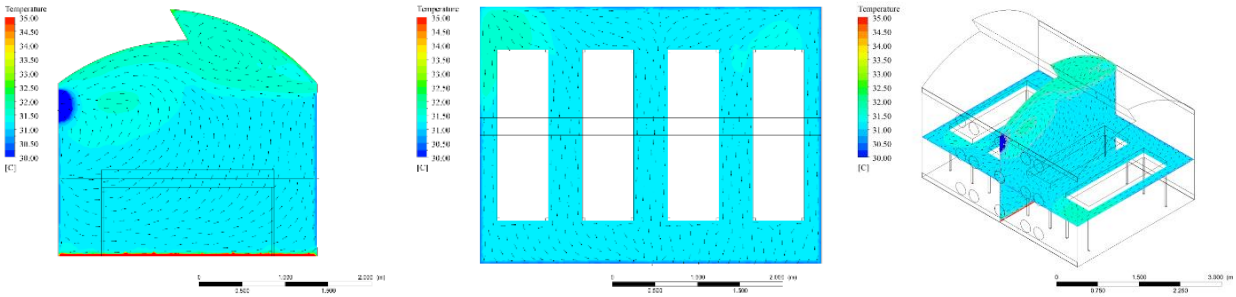

(a) Front view of greenhouse (b) Top view of greenhouse (c) Broad view

Figure 13. In the case of the top air inlet and single channel air outlet, a greenhouse-style saw tooth roof is used

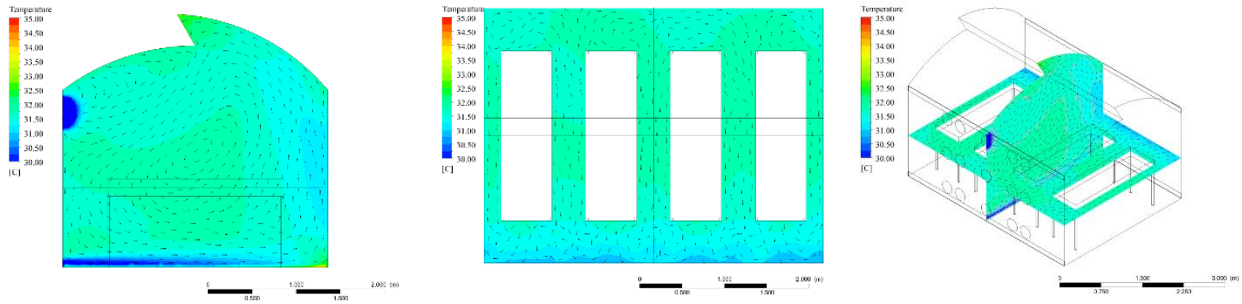

(a) Front view of greenhouse (b) Top view of greenhouse (c) Broad view

Figure 14. In the case of the air input below and the three air outputs, a greenhouse-style saw tooth roof is used.

The airflow and temperature inside an SR house are defined by natural airflow from the home and the air inlet. In the case of one air inlet and one air exit, as shown in Figure 13, the lowest mean air temperature in the dwelling was determined to be 31.21℃, which was 31.13, 31.19, and 31.32℃, respectively. According to the information provided, the third cross-section has the highest mean temperature.

In the case of the bottom air inlet shown in Figure 13 and the top three air outlets, the average temperature of the air inside the house was the highest, at 32.35℃, and the mean temperature of the cross-section was correspondingly 31.76, 32.72, and 32.66℃. Based on the above-mentioned information and the shaded colour scheme, section A had the highest average temperature.

Regarding the air turbulence shown in Figure 13(a), the direction of the arrow indicates that there are two groups of air flows, mostly upwards of the house and out via the exhaust fan channels. In the natural vent, weather and another group of air will circulate.

The top of the roof is pushed by natural air from the outside to replenish the air within the house. Figure 13(b) illustrates air flowing through the inlet line and rotating upwards as described earlier. From the findings of the house in the case of the higher air inlet and 1 upper air outlet, it is best suited for the SR house structure, while in the case of the lower air inlet and vents on 3 of Figure 14(a), the SR house structure is optimal. It was clear that hot air was moving throughout the house, particularly in the greenhouse and under the roof. Observing the shaded colour, it is clear that hot air circulates throughout the house, especially in the house and attic, where the buoyancy effect generated by the increased air temperature and humidity causes the air loop [63].

As a result, a guideline has been created to examine the influence of various rear wall vent sizes on temperature reduction in the home, particularly at the crop bed level, air flow by arrow considerations. Figure 14 (b) depicts a revolving function in the front and back of the crop bed, as well as a high heat shade in the home's center. Consequently, these greenhouses are inappropriate for usage. One or more roof vents should be designed to drain excessive heat under severe circumstances [64].

4. CONCLUSIONS

The CFD model used in this study is an effective forecasting device. Consideration of airflow and heat dissipation inside the

house to create optimal agricultural conditions in Northeast Thailand. Developed a model of the environment, the most significant model of climate change based on airflow, temperature, and distribution of weather variables necessary to enter information into the system, which is significantly influenced by the design of the house. Airflow patterns and radiation levels were shown that a direct relationship with the position of inlet and outlet vents, heat dissipation, and the mean interior temperature values. Similarly, the average temperatures of four houses varied between 30,4 and 34.1 °C. In conclusion, the findings of the research of the difference in roof shape which regulates the rate of airflow from the exhaust fan system in the form of Gable Roof (GR) continuous air flow and Curved Roof (CR), Saw tooth roof (SR), and Double roof (DR) respectively.

ACKNOWLEDGMENT

This work was supported by the Agricultural Machinery and Postharvest Technology Innovation Center, Science, Research and Innovation Promotion and Utilization Division, Office of the Ministry of Higher Education, Science, Research and Innovation and Faculty of Engineering, Khon Kaen University.

REFERENCES

[1] FAO. (2021). The state of food security and nutrition in the world. https://www.fao.org/3/cb4474en/online/cb4474en.html#chapter-1-introduction. (20/3/2022).

[2] Said Mohamed, E., Belal, A., Kotb Abd-Elmabod, S., El-Shirbeny, M.A., Gad, A., Zahran, M.B. (2021). Smart farming for improving agricultural management. The Egyptian Journal of Remote Sensing and Space Science, 24(3): 971-981. https://doi.org/10.1016/j.ejrs.2021.08.007

[3] Rabbi, B., Chen, Z.H., Sethuvenkatraman, S. (2019). Protected cropping in warm climates: A review of humidity control and cooling methods. Energies, 12(14): 2737. https://doi.org/10.3390/en12142737

[4] Liu, R. Wang, H. Guzman, J.L., Li, M. (2022). A model-based methodology for the early warning detection of cucumber downy mildew in greenhouses: An experimental evaluation. Computers and Electronics in Agriculture, 194: 106751. https://doi.org/10.1016/j.compag.2022.106751

[5] Tsafaras, I., Campen, J.B., Stanghellini, C., et al. (2021). Intelligent greenhouse design decreases water use for evaporative cooling in arid regions. Agricultural Water Management, 250: 106807. https://doi.org/10.1016/j.agwat.2021.106807

[6] Zhou, D., Meinke, H., Wilson, M., Marcelis, L.F.M., Heuvelink, E. (2021). Towards delivering on the sustainable development goals in greenhouse production systems. Resources, Conservation and Recycling, 169: 105379. https://doi.org/10.1016/j.resconrec.2020.105379

[7] Molina-Aiz, F.D., Fatnassi, H., Boulard, T., Roy, J.C., Valera, D.L. (2010). Comparison of finite element and finite volume methods for simulation of natural ventilation in greenhouses. Computers and Electronics in Agriculture, 72(2): 69-86. https://doi.org/10.1016/j.compag.2010.03.002

[8] Fidaros, D.K., Baxevanou, C.A., Bartzanas, T., Kittas, C. (2010). Numerical simulation of thermal behavior of a ventilated arc greenhouse during a solar day. Renewable Energy, 35(7): 1380-1386. https://doi.org/10.1016/j.renene.2009.11.013

[9] Villagrán, E., Flores-Velazquez, J., Akrami, M., Bojacá, C. (2021). Influence of the height in a colombian multi-tunnel greenhouse on natural ventilation and thermal behavior: Modeling approach. sustainability, 13(24): 13631. https://doi.org/10.3390/su132413631

[10] Saberian, A., Sajadiye, S.M. (2019). The effect of dynamic solar heat load on the greenhouse microclimate using CFD simulation. Renewable Energy, 138: 722-737. https://doi.org/10.1016/j.renene.2019.01.108

[11] Xu, K., Guo, X., He, J., Yu, B., Tan, J., Guo, Y. (2022). A study on temperature spatial distribution of a greenhouse under solar load with considering crop transpiration and optical effects. Energy Conversion and Management, 254: 115277. https://doi.org/10.1016/j.enconman.2022.115277

[12] Bojaca, C.R., Gil, R., Cooman, A. (2009). Use of geostatistical and crop growth modelling to assess the variability of greenhouse tomato yield caused by spatial temperature variations. Computers and Electronics in Agriculture, 65(2): 219-227. https://doi.org/10.1016/j.compag.2008.10.001

[13] Rodriguez, C.E.A., Velazquez, J.F. (2019). CFD simulation of heat and mass transfer for climate control in greenhouses. In (Ed.), Heat and Mass Transfer - Advances in Science and Technology Applications. IntechOpen. https://doi.org/10.5772/intechopen.86322

[14] Hou, Y., Li, A., Li, Y., et al. (2021). Analysis of microclimate characteristics in solar greenhouses under natural ventilation. In Building Simulation, 14(6): 1811-1821. https://doi.org/10.1007/s12273-021-0771-1

[15] Singh, M.C., Sharma, K.K., Prasad, V. (2022). Impact of ventilation rate and its associated characteristics on greenhouse microclimate and energy use. Arabian Journal of Geosciences, 15(3): 288. https://doi.org/10.1007/s12517-022-09587-1

[16] McCartney, L., Orsat, V., Lefsrud, M.G. (2018). An experimental study of the cooling performance and airflow patterns in a model Natural Ventilation Augmented Cooling (NVAC) greenhouse. Biosystems Engineering, 174: 173-189. https://doi.org/10.1016/j.biosystemseng.2018.07.005

[17] Ali, R.B., Bouadila, S., Mami, A. (2020). Experimental validation of the dynamic thermal behavior of two types of agricultural greenhouses in the Mediterranean context. Renewable Energy, 147: 118-129. https://doi.org/10.1016/j.renene.2019.08.129

[18] Choab, N., Allouhi, A., El Maakoul, A., Kousksou, T., Saadeddine, S., Jamil, A. (2019). Review on greenhouse microclimate and application: Design parameters, thermal modeling and simulation, climate controlling technologies. Solar Energy, 191: 109-137. https://doi.org/10.1016/j.solener.2019.08.042

[19] Vieira Neto, J.G., Soriano, J. (2020). Computational modelling applied to predict the pressure coefficients in deformed single arch-shape greenhouses. Biosystems Engineering, 200: 231-245. https://doi.org/10.1016/j.biosystemseng.2020.10.003

[20] Lalmi, D., Benseddik, A., Bensaha, H., Bouzaher, M.T., Arrif, T., Guermoui, M., Rabehi, A. (2021). Evaluation

and estimation of the inside greenhouse temperature, numerical study with thermal and optical aspect. International Journal of Ambient Energy, 42(11): 1269-1280. https://doi.org/10.1080/01430750.2019.1594369
[21] Villagran, E., Flores-Velazquez, J., Bojaca, C., Akrami, M. (2021). Evaluation of the microclimate in a traditional colombian greenhouse used for cut flower production. Agronomy, 11: 1330. https://doi.org/10.3390/agronomy11071330
[22] Moghaddam, J.J. (2021). The effect of turbulence on natural ventilation of a proposed octagonal greenhouse in a transient flow. International Journal of Environmental Science and Technology, 18(8): 2181-2196. https://doi.org/10.1007/s13762-020-02955-y
[23] Pakari, A., Ghani, S. (2019). Airflow assessment in a naturally ventilated greenhouse equipped with wind towers: Numerical simulation and wind tunnel experiments. Energy and Buildings, 199: 1-11. https://doi.org/10.1016/j.enbuild.2019.06.033
[24] Liu, X., Wu, X., Xia, T., Fan, Z., Shi, W., Li, Y., Li, T. (2022). New insights of designing thermal insulation and heat storage of Chinese solar greenhouse in high latitudes and cold regions. Energy, 242: 122953. https://doi.org/10.1016/j.energy.2021.122953
[25] Zhang, Y., Yasutake, D., Hidaka, K., Kitano, M., Okayasu, T. (2020). CFD analysis for evaluating and optimizing spatial distribution of CO_2 concentration in a strawberry greenhouse under different CO_2 enrichment methods. Computers and Electronics in Agriculture, 179: 105811. https://doi.org/10.1016/j.compag.2020.105811
[26] Ouammi, A., Zejli, D. (2022). Centralized controller for the optimal operation of a cooperative cluster of connected microgrids powered multi-greenhouses. Sustainable Computing: Informatics and Systems, 33: 100641. https://doi.org/10.1016/j.suscom.2021.100641
[27] Ben Amara, H., Bouadila, S., Fatnassi, H., Arici, M., Allah Guizani, A. (2021). Climate assessment of greenhouse equipped with south-oriented PV roofs: An experimental and Computational Fluid Dynamics study. Sustainable Energy Technologies and Assessments, 45: 101100. https://doi.org/10.1016/j.seta.2021.101100
[28] Chu, C.R., Lan, T.W. (2019). Effectiveness of ridge vent to wind-driven natural ventilation in monoslope multi-span greenhouses. Biosystems Engineering, 186: 279-292. https://doi.org/10.1016/j.biosystemseng.2019.08.006
[29] Shamshiri, R.R., Bojic, I., van Henten, E., Balasundram, S.K., Dworak, V., Sultan, M., Weltzien, C. (2020). Model-based evaluation of greenhouse microclimate using IoT-Sensor data fusion for energy efficient crop production. Journal of Cleaner Production, 263: 121303. https://doi.org/10.1016/j.jclepro.2020.121303
[30] Guo, Y., Zhao, H., Zhang, S., Wang, Y., Chow, D. (2021). Modeling and optimization of environment in agricultural greenhouses for improving cleaner and sustainable crop production. Journal of Cleaner Production, 285: 124843. https://doi.org/10.1016/j.jclepro.2020.124843
[31] Gorjian, S., Calise, F., Kant, K., et al. (2020). A review on opportunities for implementation of solar energy technologies in agricultural greenhouses. Journal of Cleaner Production, 285: 124807. https://doi.org/10.1016/j.jclepro.2020.124807
[32] Mazzeo, D., Baglivo, C., Panico, S., Congedo, P.M. (2021). Solar greenhouses: Climates, glass selection, and plant well-being. Solar Energy, 230: 222-241. https://doi.org/10.1016/j.solener.2021.10.031
[33] Xu, F., Lu, H., Chen, Z., Guan, Z., Chen, Y., Shen, G., Jiang, Z. (2021). Selection of a Computational Fluid Dynamics (CFD) model and its application to greenhouse pad-fan cooling (PFC) systems. Journal of Cleaner Production, 302: 127013. https://doi.org/10.1016/j.jclepro.2021.127013
[34] Zhang, X., Lv, J., Dawuda, M.M., et al. (2019). Innovative passive heat-storage walls improve thermal performance and energy efficiency in Chinese solar greenhouses for non-arable lands. Solar Energy, 190: 561-575. https://doi.org/10.1016/j.solener.2019.08.056
[35] Liu, X., Li, H., Li, Y., Yue, X., Tian, S., Li, T. (2020). Effect of internal surface structure of the north wall on Chinese solar greenhouse thermal microclimate based on Computational Fluid Dynamics. Plos One, 15(4): e0231316. https://doi.org/10.1371/journal.pone.0231316
[36] Wu, X., Liu, X., Yue, X., Xu, H., Li, T., Li, Y. (2021). Effect of the ridge position ratio on the thermal environment of the Chinese solar greenhouse. Royal Society Open Science, 8(5): 201707. http://doi.org/10.1098/rsos.201707
[37] Zhang, G., Choi, C., Bartzanas, T., Lee, I.B., Kacira, M. (2018). Computational fluid dynamics (CFD) research and application in Agricultural and biological engineering. Computers and Electronics in Agriculture, 149: 1-2. https://doi.org/10.1016/j.compag.2018.04.007
[38] Rocha, G.A.O., Pichimata, M.A., Villagran, E. (2021). Research on the microclimate of protected agriculture structures using numerical simulation tools: A technical and bibliometric analysis as a contribution to the sustainability of under-cover cropping in tropical and subtropical countries. Sustainability, 13: 10433. https://doi.org/10.3390/su131810433
[39] Kim, R., Kim, J., Lee, I., Yeo, U., Lee, S., Decano-Valentin, C. (2021). Development of three-dimensional visualisation technology of the aerodynamic environment in a greenhouse using CFD and VR technology, part 1: Development of VR a database using CFD. Biosystems Engineering, 207: 33-58. https://doi.org/10.1016/j.biosystemseng.2021.02.017
[40] Piscia, D., Muñoz, P., Panadès, C., Montero, J.I. (2015). A method of coupling CFD and energy balance simulations to study humidity control in unheated greenhouses. Computers and Electronics in Agriculture, 115: 129-141. https://doi.org/10.1016/j.compag.2015.05.005
[41] Kim, K., Yoon, J.Y., Kwon, H.J., et al. (2008). 3-D CFD analysis of relative humidity distribution in greenhouse with a fog cooling system and refrigerative dehumidifiers. Biosystems Engineering, 100(2): 245-255. https://doi.org/10.1016/j.biosystemseng.2008.03.006
[42] Li, H., Li, Y., Yue, X., Liu, X., Tian, S., Li, T. (2020). Evaluation of airflow pattern and thermal behavior of the arched greenhouses with designed roof ventilation scenarios using CFD simulation. PloS one, 15(9): e0239851. https://doi.org/10.1371/journal.pone.0239851
[43] He, X., Wang, J., Guo, S., Zhang, J., Wei, B., Sun, J., Shu, S. (2018). Ventilation optimization of solar greenhouse with removable back walls based on CFD. Computers and Electronics in Agriculture, 149: 16-25. https://doi.org/10.1016/j.compag.2017.10.001

[44] Piscia, D., Montero, J.I., Baeza, E., Bailey, B.J. (2012). A CFD greenhouse night-time condensation model. Biosystems Engineering, 111(2): 141-154. https://doi.org/10.1016/j.biosystemseng.2011.11.006
[45] Guo, J., Liu, Y., Lü, E. (2019). Numerical simulation of temperature decrease in greenhouses with summer water-sprinkling roof. Energies, 12(12): 2435. https://doi.org/10.3390/en12122435
[46] Molina-Aiz, F.D., Valera, D.L., Pena, A.A., Alvarez, A.J., Gil, J.A. (2006). Analysis of the effect of rollup vent arrangement and wind speed on Almería-type greenhouse ventilation performance using Computational Fluid Dynamics. International Symposium on Greenhouse Cooling, 719: 173-180. https://doi.org/10.17660/ActaHortic.2006.719.17
[47] Akpenpuun, T., Mijinyawa, Y. (2020). Impact of a split-gable greenhouse microclimate on the yield of irish potato (solanum tuberosum L.) under tropical conditions. Journal of Agricultural Engineering and Technology, 25(1): 54-78.
[48] Benni, S., Tassinari, P., Bonora, F., Barbaresi, A., Torreggiani, D. (2016). Efficacy of greenhouse natural ventilation: Environmental monitoring and CFD simulations of a study case. Energy and Buildings, 125: 276-286. https://doi.org/10.1016/j.enbuild.2016.05.014
[49] Bournet, P.E., Boulard, T. (2010). Effect of ventilator configuration on the distributed climate of greenhouses: A review of experimental and CFD studies. Computers and Electronics in Agriculture, 74(2): 195-217. https://doi.org/10.1016/j.compag.2010.08.007
[50] Ospina, R., Marmolejo-Ramos, F. (2019). Performance of Some Estimators of Relative Variability. Frontiers in Applied Mathematics and Statistics, 5: 43. https://doi.org/10.3389/fams.2019.00043
[51] Tanny, J. (2013). Microclimate and evapotranspiration of crops covered by agricultural screens: A review. Biosystems Engineering, 114(1): 26-43. https://doi.org/10.1016/j.biosystemseng.2012.10.008
[52] Yu, S., Yu, P., Tang, T. (2018). Effect of thermal buoyancy on flow and heat transfer around a permeable circular cylinder with internal heat generation. International Journal of Heat and Mass Transfer, 126: 1143-1163. https://doi.org/10.1016/j.ijheatmasstransfer.2018.06.056
[53] Nebbali, R., Roy, J.C., Boulard, T. (2012). Dynamic simulation of the distributed radiative and convective climate within a cropped greenhouse. Renewable Energy, 43: 111-129. https://doi.org/10.1016/j.renene.2011.12.003
[54] Ghernaout, B., Bouabdallah, S., Atia, A., Arıcı, M. (2021). Heat and fluid flow in an open agricultural greenhouse in presence of plants. Advances in Modelling and Analysis B, 64(1-4): 1-8. https://doi.org/10.18280/ama_b.641-401
[55] Bjerg, B., Cascone, G., Lee, I.B., et al. (2013). Modelling of ammonia emissions from naturally ventilated livestock buildings. Part 3: CFD modelling. Biosystems Engineering, 116(3): 259-275. https://doi.org/10.1016/j.biosystemseng.2013.06.012
[56] Poojeera, S., Srichat, A., Naphon, N., Naphon, P. (2022). Study on thermal performance of the small-scale air conditioning with thermoelectric cooling module. Mathematical Modelling of Engineering Problems, 9(4): 1143-1151. https://doi.org/10.18280/mmep.090434
[57] Maouedj, R., Youcef, A. (2020). Impact of twisted fins on the overall performances of a rectangular-channel air-heat exchanger. Mathematical Modelling of Engineering Problems, 7(3): 335-344. https://doi.org/10.18280/mmep.070302
[58] Bartzanas, T., Kacira, M., Zhu, H., et al. (2013). Computational Fluid Dynamics applications to improve crop production systems. Computers and Electronics in Agriculture, 93: 151-167. https://doi.org/10.1016/j.compag.2012.05.012
[59] Bournet, P.E., Chassériaux, G., Winiarek, V. (2006). Simulation of Energy Transfers in a Partitioned Glasshouse during. Daytime using a Bi-Band Radiation Model.. Acta Horticulturae, 719: 357-364. https://doi.org/10.17660/ActaHortic.2006.719.40
[60] Bartzanas, T., Boulard, T., Kittas, C. (2004). Effect of Vent Arrangement on Windward Ventilation of a Tunnel Greenhouse. Biosystems Engineering, 88(4): 479-490. https://doi.org/10.1016/j.biosystemseng.2003.10.006
[61] Andersen, K.T. (2003). Theory for natural ventilation by thermal buoyancy in one zone with uniform temperature. Building and Environment, 38(11): 1281-1289. https://doi.org/10.1016/S0360-1323(03)00132-X
[62] Villagran Munar, E.A., Bojacá Aldana, C.R. (2019). CFD simulation of the increase of the roof ventilation area in a traditional Colombian greenhouse: effect on air flow patterns and thermal behavior. International Journal of Heat and Technology, 37(3): 881-892. https://doi.org/10.18280/ijht.370326
[63] De la Torre-Gea, G., Soto-Zarazúa, G.M., López-Crúz, I., Torres-Pacheco, I., Rico-García, E. (2011). Computational Fluid Dynamics in greenhouses: A review. African Journal of Biotechnology, 10(77): 17651-17662. https://doi.org/10.5897/ajb10.2488
[64] Akrami, M., Javadi, A.A., Hassanein, M.J., Farmani, R., Dibaj, M., Tabor, G.R., Negm, A. (2020). Study of the effects of vent configuration on mono-span greenhouse ventilation using Computational Fluid Dynamics. Sustainability, 12(3): 986. https://doi.org/10.3390/su12030986